ChemComm

Accepted Manuscript

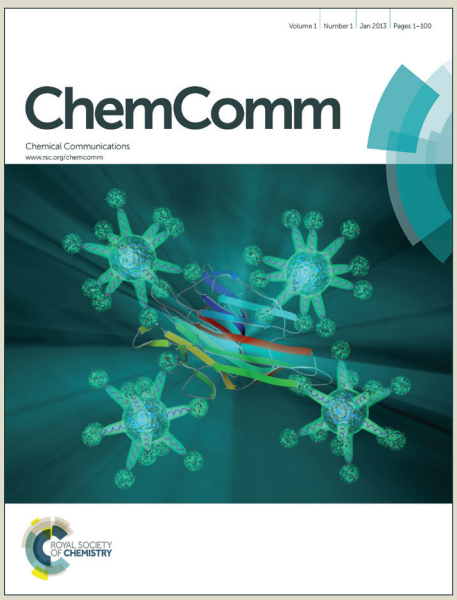

ROYAL SOCIETY OF CHEMISTRY

www.rsc.org/chemcomm

Journal Name

RSCPublishing

COMMUNICATION

Binder-free CNT network/MoS_2 composite as high performance anode material in lithium ion battery

Cite this: DOI: 10.1039/x0xx00000x

Congxiang Lu,[ab]† Wen-wen Liu[b]†, Hong Li[c] and Beng Kang Tay[*ab]

Received 00th January 2012,
Accepted 00th January 2012

DOI: 10.1039/x0xx00000x

www.rsc.org/

Carbon nanotube (CNT) network and molybdenum disulfide (MoS_2) are rationally architected into a novel type of anode material in lithium ion battery (LIB), without the necessity for any binders. Enhanced structural stability and reaction kinetics enable its high and stable capacity as well as superior rate capability.

Lithium ion batteries (LIBs) nowadays serve as the most important power source for portable electronics and are also identified as a promising power solution for future electric vehicles.[1] However, development of LIBs is now bottlenecked by the graphite anodes, due to their limited specific capacity of 372 mAh/g. As such, novel anode materials with higher capacity without compromising the cyclability have become the subject of intensive research worldwide. Among the emerging materials, MoS_2 has attracted particular attention, because of much smaller volumetric changes in the lithiation/de-lithiation processes.[2-14] Therefore, it could provide the potential for less degradation during cycling and better rate capability.

However, the performances of anodes made of bulk MoS_2 materials are still far from ideal, providing only limited capacities and suffering from severe capacity fading. One reason is their intrinsically poor electric and ionic conductivities which hinder efficient charge transfer.[6] Besides, the typical conversion of MoS_2 to Li_2S and Mo happening during lithiation[3, 15] is likely to degrade the electrodes, if no anchoring sites are provided. In addition, in bulk forms of MoS_2, capacities are often significantly constrained due to the difficulty for internal portion of the material to be fully lithiated.

Making MoS_2 into nanostructures and compositing them with other nano materials, especially those from carboneous family like graphene[3, 5, 10, 11] or CNTs[4, 6-8, 16] are considered as promising solutions for the problems. CNTs exhibit superior properties such as excellent electrical,[17] thermal conductivity[18] and structural stability.[19, 20] Therefore, it is expected that by combining the merits of CNT and MoS_2, the CNT/MoS_2 composite can be a promising anode material in LIBs. Highly conductive CNTs facilitate charge transfer during cycling while their hollowed structure and mechanical strength enable them to be excellent volume buffer for MoS_2 during lithiation/de-lithiation.

There have been a number of reports on the synthesis of CNT/MoS_2 composites.[2, 4, 8] It may be noteworthy that although the synthesis methods as well as morphology control of such composites definitely play significant roles in the performance, yet, how the material is assembled onto the current collector may also be of high impact. In particular, direct conductive pathways constructed between active material and current collectors have proven to be beneficial to the effective charge transfer.[21, 22] However, to the best of our knowledge, there have not been such reports on CNT/MoS_2 composites so far. Active materials have to be mixed with polymer binders before electrochemical testing. If there was a method to exclude these less conductive additives, it could be a step further in the development of CNT/MoS_2 anode materials. In this regard, we develop a method to synthesize MoS_2 material on the surface of CNTs which are grown on the metal current collectors and self-assembled into networks (see ESI for experimental details). The obtained composite can be directly used for LIB testing without binders. This novel architecture exhibits greatly improved electrochemical performances including high reversible capacity, excellent capacity retention and rate capability.

Fig. 1(a) displays the CNTs successfully grown on the stainless steel (SS) substrate by CVD method. Length of the CNTs is about several tens of micrometers while the diameters are in the range of 10 to 50 nm. As shown in Fig S1 in ESI, CNTs consist of tens of walls, indicating their multi-walled characteristic. Interestingly, CNTs are self-assembled into a sparse network, leaving notable space inside, which is beneficial for the access of electrolyte and lithium ions during charge/discharge. CVD-prepared CNTs often come with hydrophobic surfaces. Thus, these obtained CNTs are treated by O_2 plasma to ensure complete wetting. As shown in the insets of Fig. 1 (a), the contact angle turns from 142 ° to below 10 ° after O_2 plasma treatment, indicating the change from super hydrophobic to hydrophilic. After hydrothermal reaction and annealing process, the surface of the CNTs is completely covered by MoS_2 nanoflakes, as

displayed in Fig. 1(b) and (c). The connection of the CNT network to the substrate is so strong that it survives from the harsh conditions during long-duration hydrothermal reaction. This is also advantageous for the stability of anode. Compared to those of bare CNTs, diameters of the composite nanowires increase to be 100 to 200 nm, but the porosity among the CNT network is still maintained to a large extent. Such structure could facilitate the electrolyte into contact with the active material and ensure all of its portions into electrochemical reactions. In TEM image of Fig. 1(d), core/shell structure of the CNT/MoS_2 nanowire is clearly presented. As indicated in the HRTEM image of Fig. 1(e), carbon layers that construct CNTs are separated by ca. 3.4 Å, matching the wall separation in multi-walled CNTs. The surrounding MoS_2 flakes consist of several (<10) layers, in between which the distance is around 6.4 Å, close to the interlayer distance of (002) plane orientation in MoS_2.[23] In addition, energy-dispersive X-ray spectroscopy (EDX) line scan (see ESI), manifests the element distribution from shell to core parts of the nanowires.

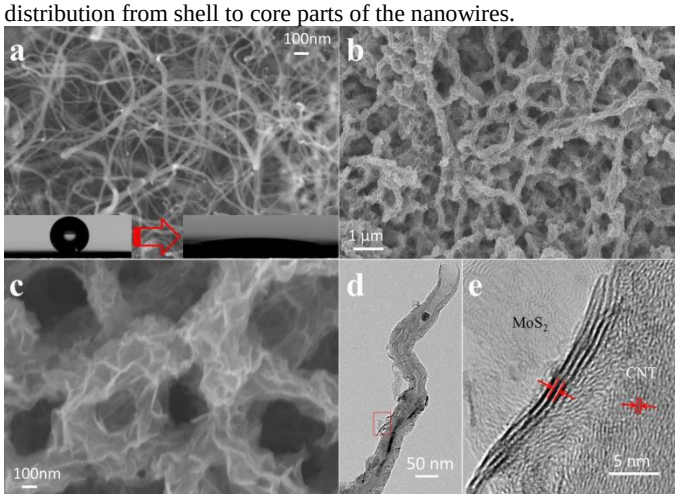

Fig. 1 (a) (b) SEM images of CNTs (insets indicate the change of contact angle by O_2 plasma treatment) and CNT/MoS_2 composite on SS substrate, respectively; (c) Higher magnification SEM image of the CNT/MoS_2 nanowires; (d) (e) TEM and HRTEM image of MoS_2 flakes on the surface of a CNT, respectively.

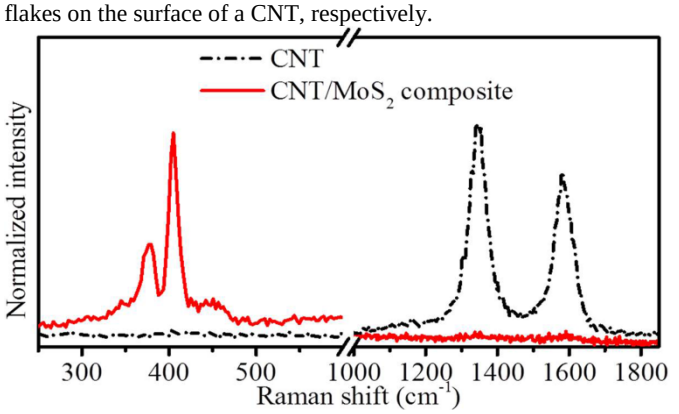

Fig. 2 Raman spectra of the CNTs (black curve) and CNT/MoS_2 composite (red curve).

Raman spectroscopy and X-ray photoelectron spectroscopy (XPS) are also employed to further characterize the CNT/MoS_2 composite. As shown in Fig. 2, the Raman spectrum of as-synthesized CNTs exhibits a G peak at 1581 cm^{-1} and a D peak at around 1347 cm^{-1}, consistent with previous reports.[2, 8, 24] After hydrothermal reaction, two characteristic peaks of MoS_2 rise at 379 and 405 cm^{-1}, which belong to the E^1_{2g} and A_{1g} modes, respectively.[25, 26] In the meantime, both D and G bands of the CNTs diminish significantly, probably due to the screening effects of the covering MoS_2 flakes.[2] Furthermore, XPS reveals that the stoichiometric ratio between Mo and S is 1:1.86, further confirming the successive synthesis of MoS_2 (see Fig S3 of ESI for details).

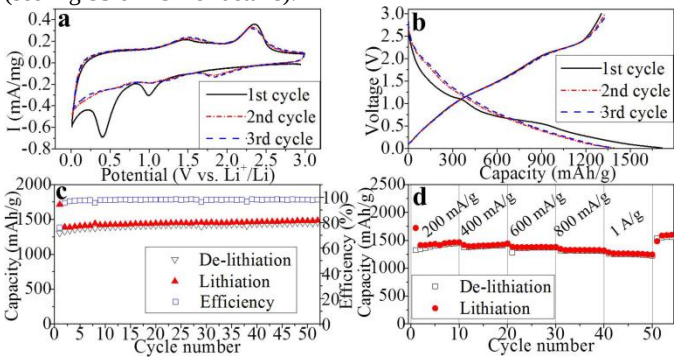

Fig. 3 (a) Cyclic voltammograms of CNT/MoS_2 composite for the first 3 cycles measured at a scan rate of 0.1 mV/s between 0.01 V and 3 V; (b) Voltage capacity profiles of CNT/MoS_2 composite at current density of 200 mA/g; (c) Specific capacities and Columbic efficiency of the CNT/MoS_2 composite versus cycle number charge/discharged at 200 mA/g; (d) Charge/discharge capacities at different current rates.

To evaluate its performance as an anode material, CNT/MoS_2 composite on SS chips is directly assembled into half cells for electrochemical testing without the usage of any binders or additives. The representative cyclic voltammetry (CV) curve for the first three cycles is shown in Fig. 3(a). In the first cycle, two distinct peaks are observed on the CV curve at 1.0 and 0.4 V, consistent with previous reports.[3, 10, 27] The cathodic peak at 1.0 V can be assigned to insertion of Li ions into the interlayer of MoS_2, transforming its phase from Mo in trigonal prismatic to Mo in octahedral coordination.[3, 7] The subsequent sharp peak located at 0.4 V is associated with the further reaction between MoS_2 and Li^+, resulting in LiS_2 and Mo metallic particles, following the reaction of $4Li+MoS_2 \rightarrow Mo+2Li_2S$.[7] It should be mentioned that both these two reduction peaks disappear in the following cycles, suggesting irreversibility in the conversion of MoS_2 into Li_2S and Mo.[9] Meanwhile, a remarkable cathodic peak appears at 1.8V, which is indicative of the lithiation process of S into Li_2S. Therefore, in the following cycles, reactions may take place between lithium and sulfur. In anodic sweeps, a broad peak around 1.5 V can be attributed to the partial oxidation of Mo to MoS_2[28] and/or de-lithiation of residual lithium intercalates (Li_XMoS_2).[2] The following pronounced peak at 2.3 V corresponds to conversion of Li_2S to S_8^{2-}.[4]

In the initial lithiation profile tested at 200 mA/g in Fig. 3(b), two voltage plateaus at around 1.1 and 0.6 V can be observed, corresponding to the formation of Li_XMoS_2 and reduction of MoS_2 into Mo particles embedded in Li_2S matrix, respectively. In the de-lithiation plots, well-defined plateaus at 2.2 V can be attributed to extraction of lithium from Li_2S. These plots are in line with aforementioned CV measurements. Initial lithiation and de-lithiation capacities at 200 mA/g of the CNT/MoS_2 composite are 1715 and 1305 mAh/g, respectively, corresponding to a columbic efficiency of 76.1%. The irreversible capacity loss of 24.9% is probably caused by formation of solid electrolyte interface (SEI), which is almost inevitable in nanosized anode materials.[29] Nevertheless, the efficiency keeps at nearly 100% in the following cycles and the composite demonstrates an impressively high de-lithiation capacity of 1456 mAh/g after 50 cycles. This is among the highest capacities as well as best cyclic performances of CNT/MoS_2 composites ever reported under the current density of 200 mA/g and also much better than the performance of commercial MoS_2 powder with binders in the control group (see Fig. S6 of ESI for details). Rate capability is

another important criterion to evaluate the performance of an anode material. As shown in Fig. 3(d), a de-lithiation capacity of 1450 mAh/g is obtained after 10 cycles at the charge/discharge current of 200 mA/g, consistent with the value in Fig. 3(c). When the current densities are raised to 400, 600, 800 and 1000 mA/g, the corresponding de-lithiation capacities are 1431, 1367, 1302 and 1224 mAh/g after 10 cycles, respectively, demonstrating high capacities and plausible cycling behavior even at high current density. Eventually, when the current is set back to 200 mA/g, the de-lithiation capacity recovers to 1535 mAh/g, indicating excellent rate capability of the composite.

The outstanding performances including high capacity, excellent cycling retention and rate capability are enabled by the rational design in material selecting, compositing and also architecting. Improved structural stability as well as efficient reaction kinetics is realized in this hierarchical assembling of CNT network and MoS_2 flakes. Firstly, the network of CNTs provides a strong skeleton for the composite, avoiding aggregation of the active material, retaining its inter-space and also large surface area to a considerable extent. Secondly, the internal cavity and flexibility of the CNTs can help to absorb or buffer the mechanical stress induced by volume variation of MoS_2 upon repetitive lithium insertion/extraction. Meanwhile, voids inside the composite not only provide space to accommodate volume change but also shorten the diffusion pathways, enabling fast Li^+ transport and hence improved rate capability. Furthermore, highly conductive CNTs are widely known as good pathways for charge transfer in nanocomposite. In this CNT network/MoS_2 flake composite, charge transfer can be further enhanced because of the direct rooting of CNT network onto the metal current collector as well as binder-free architecting.

Conclusions

In summary, an approach to fabricate binder-free CNT network/MoS_2 composite anode material has been successfully developed. It consists of CVD growth of CNTs on metal substrate and hydrothermal preparation of MoS_2 nanoflakes. Because of reinforced structural stability and also enhanced reaction kinetics, obtained CNT/MoS_2 composite demonstrates impressive electrochemical performances. Encouragingly, a high and reversible capacity over 1300 mAh/g is retained for 50 cycles at the current density of 200 mA/g, while excellent rate performance is also delivered. This method offers a new idea to optimize the CNT/MoS_2 composites under intensive research. Moreover, the binder-free constructing and usage of CVD-grown CNT network on metal substrate instead of dispersed CNTs may not be limited to CNT/MoS_2 composite. They may also be of potential for the improvement of other CNT-based composite anode materials.

Notes and references

[a] CINTRA CNRS/NTU/THALES, Nanyang Technological University, Singapore 637553.

[b] Novitas, Nanoelectronics Centre of Excellence, School of Electrical and Electronic Engineering, Nanyang Technological University, Singapore 639798.

[c] Department of Mechanical Engineering, Stanford University, California 94305, United States.

†These two authors contribute equally to this work.

The authors greatly appreciate Prof. Zhang Qing, Prof. Tan Ooi Kiang, Dr. Wang Xinghui and Ms. Luo Qiong's help in electrochemical testing and financial support from IME Si-COE project. Electronic Supplementary Information (ESI) available: See DOI: 10.1039/c000000x/

1. J. M. Tarascon and M. Armand, Nature, 2001, **414**, 359.
2. Q. Wang and J. Li, J. Phys. Chem. C, 2007, **111**, 1675.
3. K. Chang and W. Chen, ACS Nano, 2011, **5**, 4720.
4. S. J. Ding, J.S. Chen and X. W. Lou, Chem.-Eur. J., 2011, **17**, 13142.
5. H. Hwang, H. Kim and J. Cho, Nano Lett., 2011, **11**, 4826.
6. C. F. Zhang, Z. Y. Wang, Z. P. Guo and X. W. Lou, ACS Appl. Mater. Interfaces, 2012, **4**, 3765.
7. K. Bindumadhavan, S. K. Srivastava and S. Mahanty, Chem. Commun., 2013, **49**, 1823.
8. Y. M. Shi, Y. Wang, J. I. Wong, A. Y. S. Tan, C. L. Hsu, L. J. Li, Y. C. Lu and H. Y. Yang, Sci Rep, 2013, **3**, 2169.
9. T. J. Stephenson, Z. Li, B. Olsen and D. Mitlin, Energy Environ. Sci., 2014, **7**, 209.
10. K. Chang and W. Chen, Chem. Commun., 2011, **47**, 4252.
11. X. Cao, Y. Shi, W. Shi, X. Rui, Q. Yan, J. Kong and H. Zhang, Small, 2013, **9**, 3433.
12. K. Chang, W. Chen, L. Ma, H. Li, H. Li, F. Huang, Z. Xu, Q. Zhang and J.-Y. Lee, J. Mater. Chem., 2011, **21**, 6251.
13. C. Zhang, H. B. Wu, Z. Guo and X. W. Lou, Electrochem. Commun., 2012, **20**, 7.
14. X. Zhou, Z. Wang, W. Chen, L. Ma, D. Chen and J. Y. Lee, J. Power Sources, 2014, **251**, 264.
15. S. Ding, D. Zhang, J. S. Chen and X. W. Lou, Nanoscale, 2012, **4**, 95.
16. S. K. Park, S. H. Yu, S. Woo, B. Quan, D. C. Lee, M. K. Kim, Y. E. Sung and Y. Piao, Dalton Trans., 2013, **42**, 2399.
17. T. W. Ebbesen, H. J. Lezec, H. Hiura, J. W. Bennett, H. F. Ghaemi and T. Thio, Nature, 1996, **382**, 54.
18. S. Berber, Y. K. Kwon and D. Tománek, Phys. Rev. Lett., 2000, **84**, 4613.
19. M. M. J. Treacy, T. W. Ebbesen and J. M. Gibson, Nature, 1996, **381**, 678.
20. A. L. M. Reddy, M. M. Shaijumon, S. R. Gowda and P. M. Ajayan, Nano Lett., 2009, **9**, 1002.
21. H. X. Zhang, C. Feng, Y. C. Zhai, K. L. Jiang, Q. Q. Li and S. S. Fan, Adv. Mater., 2009, **21**, 2299.
22. C. M. Ban, Z. C. Wu, D. T. Gillaspie, L. Chen, Y. F. Yan, J. L. Blackburn and A. C. Dillon, Adv. Mater., 2010, **22**, E145.
23. U. K. Sen and S. Mitra, ACS Appl. Mater. Interfaces, 2013, **5**, 1240.
24. M. S. Dresselhaus, G. Dresselhaus, R. Saito and A. Jorio, Phys. Rep.-Rev. Sec. Phys. Lett., 2005, **409**, 47.
25. H. Li, Q. Zhang, C. C. R. Yap, B. K. Tay, T. H. T. Edwin, A. Olivier and D. Baillargeat, Adv. Funct. Mater., 2012, **22**, 1385.
26. A. Molina-Sanchez and L. Wirtz, Phys. Rev. B, 2011, **84**, 155413.
27. H. Liu, D. Su, R. Zhou, B. Sun, G. Wang and S. Z. Qiao, Adv. Energy Mater., 2012, **2**, 970.
28. L. C. Yang, S. N. Wang, J. J. Mao, J. W. Deng, Q. S. Gao, Y. Tang and O. G. Schmidt, Adv. Mater., 2013, **25**, 1180.
29. J. E. Owejan, J. P. Owejan, S. C. DeCaluwe and J. A. Dura, Chem. Mat., 2012, **24**, 2133.